Functional Equivalence of Metarhodopsin II and the G_t-Activating Form of Photolyzed Bovine Rhodopsin†

Julia Kibelbek, Drake C. Mitchell, James M. Beach, and Burton J. Litman*
Department of Biochemistry, University of Virginia Health Sciences Center, Charlottesville, Virginia 22908
Received December 18, 1990; Revised Manuscript Received March 20, 1991

ABSTRACT: Absorption of a photon by the visual pigment rhodopsin leads to the formation of an activated conformational state, denoted rho*, which is capable of activating the visual G-protein, G_t. The bleaching of rhodopsin can be resolved into a series of spectrally distinct photointermediates. Previous studies suggest that the photointermediate metarhodopsin II (meta II, λ_{max} of 380 nm) corresponds to the physiologically active form rho*. In the studies reported herein, spectral and enzymological data were analyzed and compared so as to evaluate the temporal correspondence between meta II and rho*. This information was obtained by direct observation of the meta II and rho* decay times in parallel experiments utilizing identical preparations of urea-stripped, bovine retinal rod outer segment disk membranes at pH 8.0, 20 °C. Postflash spectra were deconvolved to resolve the meta II absorbance at 380 nm, and a decay time for the loss of meta II of 8.2 min (SD = 0.5 min) was obtained from fitting these data to a single-exponential decay process. The diminishing ability of bleached rhodopsin to activate G_t was measured by monitoring the level of catalyzed exchange of G_t-bound GDP for a nonhydrolyzable GTP analogue. Analysis of the decrease in the initial velocity of nucleotide exchange, measured at various postflash incubation times, yielded a rho* decay time of 7.7 min (SD = 0.5 min) when analyzed as a single-exponential process. The similarity of these decay times provides direct evidence that meta II and rho* are present over the same time regime, and further supports the equivalence of these two forms of photoactivated rhodopsin. Rho* decay measurements were characterized by a residual level of G_t activation, which persisted after the dynamic phase of the rho* decay was complete. Spectral measurements, in the presence and absence of added G_t, showed G_t-induced formation of meta II from the existing pool of meta III; this demonstrates directly the reversibility of the meta II ↔ meta III equilibrium. The formation of meta II from meta III under the conditions where the residual level of rho* activity persists provides further evidence for the equivalence of these two forms of photoactivated rhodopsin.

The integral membrane protein rhodopsin belongs to a family of receptors that couple external stimuli to internal cellular responses via a G-protein (G_t)[1] linked to an effector enzyme. Absorption of a photon triggers the isomerization of rhodopsin's bound chromophore from 11-*cis*-retinal to *all-trans*-retinal and generates rho*, a transient conformation capable of activating G_t via a catalyzed exchange of G_t-bound GDP for GTP. Activated G_t effects the removal of the inhibitory γ subunits from PDE, activating the enzyme with resultant hyperpolarization of the rod cell (Fung, 1985; Stryer, 1986; Deterre et al., 1988).

The postabsorption events in rhodopsin bleaching can be resolved spectrophotometrically as a series of intermediates, each with a characteristic wavelength maximum (Matthews et al., 1963). Meta II, which is formed milliseconds after bleaching, is the last photointermediate formed on a time scale fast enough to be implicated in visual signal transduction. Meta II and its predecessor, meta I, coexist in a pH- and temperature-sensitive equilibrium, which is stable for several seconds at room temperature. Emeis and Hofmann (1981) found that for bleaches of <10% in bovine ROS suspensions, this equilibrium was shifted in favor of meta II, and concluded that this shift was caused by enhanced meta II formation due to the formation of a stable G_t·meta II complex in the absence of GTP. For bleaches >10%, where rho* would exceed G_t so that 1:1 binding is no longer possible, they observed normal meta I ↔ meta II equilibria for that rhodopsin which was in excess of the G_t concentration in the sample. Bennett et al. (1982) used light-scattering signals as an indication of light-induced G_t binding to disk membranes (Kuhn et al., 1981) to show that the initial phase of G_t binding occurs after formation of meta II (as measured by transmittance changes at 365 nm) and that conditions which lead to the onset of the binding signal also lead to enhanced meta II formation. They also found similar decay kinetics for the loss of the binding signal and the meta II → meta III transition. These results have been substantiated by additional investigations involving light scattering and enhancement of meta II formation induced by binding of G_t (Emeis et al., 1982; Hofmann, 1985). Further evidence for a correlation between the simultaneous formation of meta II and rho* was provided by experiments on rhodopsin, which was modified by methylation of the retinal–opsin Schiff base linkage; this modification arrested the photointermediate cascade at meta I and resulted in a loss of ability to stimulate GTPase activity on G_t (Longstaff et al., 1986). These effects are attributed to blocking the deprotonation of the retinal

†Supported by NIH Grant EY00548. Previous reports of this work appeared in Kibelbek et al. (1990a,b).
* Author to whom correspondence should be addressed.

[1] Abbreviations: G_t, visual G-protein, GTPase of the rod outer segment, or transducin; PDE, phosphodiesterase of the rod outer segment; meta I, metarhodopsin I; meta II, metarhodopsin II; meta III, metarhodopsin III; NRO_{365}, *N*-retinylidene opsin; Tris, tris(hydroxymethyl)aminomethane; DTPA, diethylenetriaminepentaacetic acid; DTT, dithiothreitol; EDTA, ethylenediaminetetraacetic acid; ROS, rod outer segment(s); GMPPNP, guanosine 5′-(β,γ-imidotriphosphate); V_d, initial velocity of nucleotide exchange on G_t in the dark; V_0', apparent initial velocity of rho*-catalyzed nucleotide exchange on G_t; V_0, initial velocity of rho*-catalyzed nucleotide exchange on G_t corrected for dark activity ($V_0' - V_d$); POPC, 1-palmitoyl-2-oleoyl-3-*sn*-phosphatidylcholine.

0006-2960/91/0430-6761$02.50/0

Schiff base by methylation of the Schiff base. These studies suggest that deprotonation of the protonated Schiff base is required for the formation of both meta II and rho*.

In contrast to the previous studies, Okada et al. (1989) reported stimulation of GTPase activity by post-meta II photoproducts. They detected similar levels of GTPase activity for bleached disk samples plus and minus hydroxylamine under conditions where hydroxylamine converts all photoisomerized chromophores to retinal oxime. They also measured a dark GTPase activity, which was at somewhat reduced levels relative to light-stimulated activity, with previously bleached disks that had been incubated with 11-*cis*-retinal at 0 °C in the dark, under conditions where regeneration of rhodopsin should have occurred. In apparent conflict with earlier investigations, the results of Okada et al. imply that the rho* configuration of bleached rhodopsin is completely uncoupled from the state of the chromophore, persisting after conversion of the chromophore to retinal oxime or regeneration of the pigment with 11-*cis*-retinal.

The experiments reported here consist of direct spectral measurements to monitor meta II decay carried out in conjunction with direct nucleotide exchange measurements on G_t, so as to monitor the time-dependent loss of rho* activity following an activating bleach. The goal of these measurements was to rigorously examine the extent of the temporal coincidence between meta II and rho*. Direct evidence that meta II and rho* decay in the same time domain, in conjunction with earlier findings suggesting the coincidence of their formation, would support an identity of the two species. All measurements were made on aliquots of the same preparation of urea-stripped disk membranes. The meta II decay time was obtained from a series of postflash absorbance spectra, deconvoluted to resolve the meta II absorbance. The rho* decay time was obtained by assaying bleached samples of disk membranes for their ability to catalyze nucleotide exchange on G_t at various times after bleaching. Nearly identical decay times for meta II and rho* were observed by using these direct techniques, substantiating the conclusions of earlier investigators regarding the coincidence of meta II and rho*, which were drawn from more indirect measurements. A residual nucleotide exchange activity, above the dark control levels, which persisted after the completion of the dynamic phase of the rho* decay, was consistently observed. This constant level of residual activity either suggested G_t activation by some form of bleached rhodopsin other than meta II, or suggested activation by meta II which had been formed from the meta III pool. Spectral measurements demonstrate that the addition of G_t to a sample containing predominantly meta III causes the formation of meta II with a corresponding loss of meta III. This result provides direct evidence for a reversible meta II $\leftrightarrow$ meta III equilibrium and supports a mechanism for the residual rho* activity in the decay curves wherein added G_t induces meta II formation from the meta III pool.

Materials and Methods

All manipulations were performed under dim, far-red light (Kodak Wratten no. 2) at 4 °C unless otherwise noted, and all experiments were carried out at pH 8.0, 20 °C. Isotonic buffer contains 10 mM Tris (pH 8.0), 60 mM KCl, 30 mM NaCl, 2 mM $MgCl_2$, 50 μM DTPA, 2 mM DTT, and 100 Kallikrein inhibitor units (KIU)/mL of the protease inhibitor Trasylol (Mobay Pharmaceuticals). Hypotonic buffer contains 5 mM Tris (pH 8.0), 1 mM EDTA, 2 mM DTT, and 100 KIU/mL Trasylol. All fits of asymmetric quasi-Gaussians to spectral data, linear fits of time courses of G_t activation, and fits of single exponentials to the decays of meta II and rho* were performed with nonlinear least-squares parameter estimation software which utilizes the modified Gauss–Newton algorithm developed by Johnson (Johnson, 1983; Johnson & Frasier, 1985). This software derives asymmetric confidence intervals corresponding to one standard deviation (68.3% confidence) for the fitted parameter(s), but because of the minimal observed asymmetry, a single estimate of standard deviation is reported in all cases.

Preparation of Urea-Stripped Disk Membranes. Rod outer segments were isolated from frozen bovine retinas (James and Wanda Lawson, Lincoln, NE) by the method of McDowell and Kuhn (1977) with the modifications described in Miller et al. (1986). These ROS preparations were first washed isotonically to remove soluble proteins and then hypotonically to remove PDE and G_t ("hypotonic extract", see below). At this point, the washed disks were resuspended in isotonic buffer, homogenized, and spun down at 30000 rpm in a Beckman 75Ti rotor for 15 min. The pellets were taken up in 4 M urea (pH 7.8–8.0) to a rhodopsin concentration of 1 mg/mL, resuspended and homogenized, and then spun down at 30000 rpm for 30 min. The supernatant was removed, and the urea-stripped disks were then washed twice isotonically and twice hypotonically. Total time of exposure to 4 M urea was 30 min, not including the spin. Disks prepared in this manner exhibited neither dark- nor light-stimulated nucleotide exchange activity, as measured by the nucleotide exchange assay described below. Disks were stored under argon at 4 °C and used within 2 weeks of preparation. Urea-stripped disks were used for these experiments because they contained no detectable G_t which might bind and stabilize rho* during the postflash incubation.

Preparation of Hypotonic Extract. A hypotonic extract was prepared from disks before urea stripping according to the method described in Miller et al. (1987). Three isotonic washes were carried out at 2 mg/mL rhodopsin; three hypotonic washes were carried out at 4 mg/mL rhodopsin. Hypotonic supernatants were spun at 30000 rpm for 45 min in a Beckman 50.2Ti rotor at 4 °C to remove membrane fragments, pooled, concentrated by using an Amicon PM-10 membrane, and stored at −20 °C in 30% glycerol. Hypotonic extracts were used within 2 weeks, during which the concentration of active G_t (as measured by the nucleotide exchange assay) did not decrease significantly.

Spectral Measurements. All spectral data were acquired and analyzed according to the detailed procedures outlined in Straume et al. (1990). Absorbance spectra were acquired with a Hewlett-Packard 8452A diode array spectrophotometer with a reference solution consisting of a suspension of fine white particles which closely matched the light-scattering properties of the sample. Each spectrum was corrected for any residual scattering by using a modified form of Rayleigh's equation for scattering. Samples consisted of suspensions of urea-stripped disk membranes (0.3–0.4 mg/mL rhodopsin) which were briefly sonicated under argon, in a cup sonicator filled with water at 0 °C, so as to improve optical clarity. Samples were flashed with a camera strobe which was equipped with a 520 ± 25 nm band-pass filter, resulting in a 20–25% bleach. The following sequence of spectra was recorded: (1) the initial, unbleached solution; (2) a series of postflash scans, the first of which was acquired 3 s after the bleaching flash; (3) following addition of 2 M hydroxylamine to a final concentration of 30 mM (to convert all bleached chromophores to retinal oxime) added after the series of spectra in (2) were collected; and (4) after complete bleaching of the sample in the presence of hydroxylamine. An example

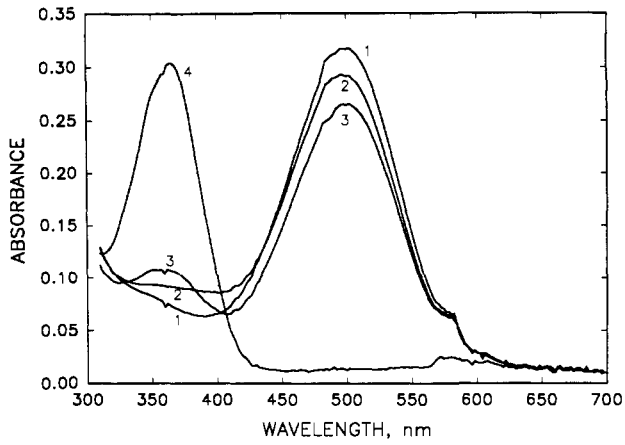

FIGURE 1: Example of the series of spectra, acquired by using a scattering blank, employed to determine the meta II decay time. Only 1 representative spectrum of the approximately 20 postflash scans collected is shown (2). (1) The initial, unbleached disk solution; (2) the first postflash scan, acquired 3 s after the flash; (3) scan following addition and complete reaction of NH_2OH; (4) scan after complete bleaching in the presence of NH_2OH.

of this series, which for clarity includes only the first of the postflash series of scans, is given in Figure 1. The series of postflash scans for analysis of the decay of meta II consisted of 20 spectra, with the first of these acquired 3 s after the photolyzing flash, and the last one acquired after ~50 min.

Analysis of Meta II Decay Time. The Hewlett-Packard 8452A reports the uncertainty corresponding to one standard deviation at each measuring wavelength. These uncertainties were linearly propagated during all analytical procedures and were used by the nonlinear parameter estimation software during deconvolution of spectra into constituent species to yield error estimates for the fitted spectra.

All measurements were made at pH 8.0. Previous studies have shown that the spectra in the timed series and Figure 1 contain varying contributions from six distinct spectral species: rhodopsin, meta I, meta II, meta III, NRO_{365}, and retinal oxime (Blazynski & Ostroy, 1981, 1984). Spectra 1, 3, and 4 in Figure 1 contain contributions from only rhodopsin and retinal oxime. The three possible difference spectra formed from these three scans were simultaneously fit to the sum of two asymmetric quasi-Gaussians: one for rhodopsin and one for retinal oxime. In this manner, the initial concentration of rhodopsin, the fraction of the sample bleached, and the location and band shape of the rhodopsin and retinal oxime absorption peaks were obtained. The spectrum of the initial sample (Figure 1, spectrum 1) was then subtracted from each of the postflash spectra, and the resulting difference spectra were corrected for unbleached rhodopsin by using the band shape derived for rhodopsin as described above. These corrected difference spectra consisted of absorbance due only to the photochemical intermediates present from 3-s to 50-min postflash. The first corrected difference spectrum of the postflash series (acquired 3-s postflash) contained only meta I and meta II, and the band shapes of these two species were derived by fitting the sum of two asymmetric quasi-Gaussians to this spectrum. The concentrations of meta I and meta II in the 3-s postflash scan were determined by using extinction coefficients for these two species of 44 000 and 38 000 M^{-1} cm^{-1}, respectively (Applebury, 1984). The accuracy of deconvolving the 3-s postflash scan into meta I and meta II was ascertained by comparing the sum of the meta I and meta II concentrations with the concentration of bleached rhodopsin. Above pH 7.7, the bleached chromophore hydrolyzes to NRO_{365} (Blazynski & Ostroy 1981, 1984); thus, the final spectrum of the postflash series was modeled as a mixture of meta III and NRO_{365}. The band shapes of these two species were derived in the same manner as those for meta I and meta II, and the concentrations of meta III and NRO_{365} in the final postflash scan were determined by using extinctions of 42 000 and 33 000 M^{-1} cm^{-1}, respectively (Blazynski & Ostroy, 1981). The accuracy of deconvolving the last postflash scan into meta III and NRO_{365} was judged by comparing the sum of the meta III and NRO_{365} concentrations with the concentration of bleached rhodopsin. The ratios meta II/meta I and meta III/NRO_{365} are expected to remain constant during the decay process; thus, all spectra acquired at intermediate times were fit with linear combinations of the derived meta I–meta II and NRO_{365}–meta III band shapes, as shown in eq 1. All spectra

spectra at intermediate times =

$$\alpha(\text{meta I–meta II spectrum derived from 3-s scan}) + \beta(\text{meta III–NRO}_{365}\text{ spectrum derived from last scan}) \quad (1)$$

from intermediate times were deconvolved into contributions due to meta I, meta II, meta III, and NRO_{365} by varying only α and β in eq 1; individual band shapes and wavelength maxima for these four species were held constant at their previously determined values. The accuracy of this procedure for deconvolving the intermediate spectra into the four photointermediate species was judged by comparing the sum of their concentrations with the concentration of bleached rhodopsin.

The meta II decay time (time to fall to $1/e$ of the initial value) was derived from the time-dependent loss of intensity at the absorbance maximum of the meta II spectrum which was deconvoluted from each scan of the series of postflash corrected difference spectra. Uncertainties in the individual meta II absorbance maxima, corresponding to one standard deviation, were derived by appropriately combining the standard deviations of α and the meta II absorbance maximum derived from the 3-s scan. Nonlinear least squares was used to fit a single-exponential decay to the deconvolved maximum meta II absorbance as a function of time after the bleaching flash. Hence, the meta II decay time is determined by a process which includes a global fit of the entire deconvoluted meta II spectrum, as opposed to using the observed change in absorbance at a single wavelength such as 380 nm. The meta II decay time was obtained in this way for each of four separate postflash series of spectra. The final value of the meta II decay time was obtained by averaging the values of the four independent experiments, weighted by their standard deviations.

Effect of G_t on Meta II–Meta III. Spectral measurements, to determine the ability of G_t to influence the amount of meta II which is in dynamic equilibrium with meta III, were carried out in a manner similar to the measurements of meta II decay. The first postflash scan was acquired 3 s after the bleaching flash, and was used to determine the amounts of meta I and meta II formed as a result of photolysis. The sample was then incubated at 20 °C in the dark for ca. 50 min and scanned again. This scan was used to determine the unperturbed amounts of meta III and NRO_{365} formed. Following this incubation period, the sample was divided in half, and hypotonic extract (0.8 G_t/bleached rhodopsin) was added to half of the photolyzed sample and hypotonic extract buffer without G_t was added to the other half. The samples were allowed to incubate in the dark for 10 min; then both samples were scanned every 2 or 3 min over a 20-min period. Finally, both samples were scanned following the addition of hydroxylamine and after complete bleaching, the equivalent of spectra 3 and 4, respectively, of Figure 1. Corrected difference spectra were

created from all scans as described under Analysis of Meta II Decay Time.

Nucleotide Exchange Measurements and Analysis. The rho* decay time was derived by assaying the time-dependent loss of ability of a sample of bleached rhodopsin to catalyze nucleotide exchange on G_t. After initial bleaching, a sample of urea-stripped disks was stored in the dark for times ranging from 45 s to about 5 h. This is referred to as the "postflash incubation time", and during this time, the rho* formed by the bleach underwent thermal decay. Rho* activity in each of these incubated samples was derived from the nucleotide exchange assay in the following way. At the completion of the minus G_t, postflash incubation time, the disk sample was mixed with a suspension of hypotonic extract (containing G_t) and [^{3}H]GMPPNP, and the rho*-catalyzed exchange of GDP for GMPPNP on G_t was assayed every ca. 3 min for 20 min: these nucleotide exchange assays are referred to as nucleotide exchange "time courses". The initial velocity of each GDP–GMPPNP exchange reaction, V_0, was determined by subtracting the exchange velocity in the dark, V_d, from V_0', the apparent initial exchange velocity for that reaction. The initial velocity of the nucleotide exchange reaction, V_0, is proportional to the rho* activity. The concentration of G_t in these experiments was >150 times that of the initial rho*. Thus, it was assumed that once the mixing of the disk sample and the hypotonic extract took place, there would be sufficient excess G_t relative to rho* to bind any available rho* and prevent appreciable further thermal decay throughout the period over which V_0' was measured. A more detailed description of the experimental procedure follows.

Aliquots of urea-stripped disk membrane suspensions (0.45 mg/mL rhodopsin) were bleached with a calibrated flash of light. A single camera strobe flash of 1-ms duration, attenuated with neutral density filters to achieve a constant bleach level for a given experiment, was employed. The bleach level varied from 0.11 to 0.33% depending on the experiment. An infrared lamp and image converter were used for all sample manipulation. After the activating flash, each sample was incubated in the dark in the absence of G_t at 20 °C. At the end of each selected postflash incubation time, an aliquot of the flashed sample was added to a mixture of hypotonic extract containing G_t and GMPPNP to final concentrations of 2.5 μM rhodopsin, 1.1–1.4 μM G_t, and 10 μM GMPPNP spiked with [^{3}H]GMPPNP at a specific activity of $\sim 1 \times 10^{15}$ dpm/mol. In continued darkness, a nitrocellulose filter binding time course assay was immediately performed so as to measure the extent of nucleotide exchange on G_t [Fung & Stryer (1980) with the modifications described in Miller et al. (1989)]. Time points were selected over a range from 0 to 20 min so as to yield the nucleotide exchange time course. In these assays, nucleotide bound to G_t is retained on the filter, whereas unbound nucleotide is rinsed off. Each of these nucleotide exchange time courses contained five or six time points (each taken in triplicate), separated by 3–4 min. After the last time point, each sample was bleached completely with a microscope light for about 3 min, and triplicate aliquots were subjected to the nucleotide exchange assay to determine maximum exchange for that sample. The maximum nucleotide exchange values for the final time point of these samples agreed with the expected values for maximum G_t activation based upon a previous nucleotide exchange assay of G_t in the hypotonic extract. The average maximum G_t activation was 1.33 μM (SD = 0.08 μM) for the first rho* decay experiment and 1.12 μM (SD = 0.04 μM) for the second. The small standard deviation for both of these numbers indicates that for a given experiment the individual nucleotide exchange time course samples contained the same amount of G_t and that comparisons of individual initial velocities of G_t activation are valid.

All nucleotide exchange assay results were quantified by counting the radioactivity retained on the filter using aliquots of the GMPPNP stock spiked with [^{3}H]GMPPNP as a calibration standard. Data for individual points in the time course consisted of the average of a triplicate sample. Each point was normalized to percent of maximum exchange. For all subsequent analysis and graphical representation, the standard deviation of the triplicate sample was taken as the uncertainty for each time course data point. Time courses are plotted as percent of maximum nucleotide exchanged, or percent of maximum G_t activated, versus minutes after mixing. Data from unflashed, dark controls were fit with a line, the slope of which, V_d, represents the velocity of G_t activation in the absence of catalysis by rho*. Data from time courses containing flashed rhodopsin are not necessarily linear over the span of the whole 20 min, since they represent enzyme-catalyzed reactions. In order to determine V_0', the apparent initial velocity of G_t activation, a series of linear fits was carried out in the initial region of each time course. The number of data points in the initial region of the time course considered suitable for determining V_0' was such that the variance of the fit to these points did not exceed the variance of the dark control linear fits by more than 10%. All linear fits were carried out by using a least-squares fitting program, and the number of points used to fit a time course ranged from 2 to 5, with the number of points in the fit generally increasing with longer postflash incubation times. In order to determine the actual initial velocity, V_0, for each time course, V_d was subtracted from V_0'. The standard deviations of V_d and V_0' were determined by the least-squares fitting program, and these were linearly propagated to obtain the standard deviation of V_0. Values of V_0 (units are change in percent maximum exchange/minute) were plotted as a function of postflash incubation time and were fit with a single-exponential decay to yield the value of the rho* decay time, with a standard deviation determined by the nonlinear least-squares program. The results of two independent determinations of the decay time of rho* were averaged, weighted by their standard deviations, to produce the final decay time value.

Results

Meta II Decay Time. The meta II decay time was determined by recording a series of postflash spectra over a period from 3 s to about 50 min and deconvolving the contribution of the various photointermediates present. The change in the mixture of photointermediates with time is demonstrated by the four postflash corrected difference spectra shown in Figure 2, where for clarity only four of the typical series of 20 postflash spectra are presented. This figure clearly shows an increase in absorbance at 465 nm due to the formation of meta III and a concomitant decrease in absorbance at 380 nm due to the decay of meta II, as well as the resulting isosbestic point at 422 nm. The corrected difference spectra acquired 3-s and 50-min postflash were well described by a combination of meta I and meta II, and meta III and NRO_{365}, respectively, as shown in Figure 3A,B. At 3-s postflash, the ratio of meta II to meta I was found to have a value of 0.71 ± 0.05 (n = 6), in good agreement with the value of 0.75 reported by Parkes and Liebman (1984) for disks at pH 8, 20 °C. At 50-min postflash, the mixture of meta III and NRO_{365} was found to consist of 71% meta III (±6%, n = 6), consistent with the report of Blazynski and Ostroy (1981, 1984) that 70–75% of meta II decays via meta III at pH 8.0.

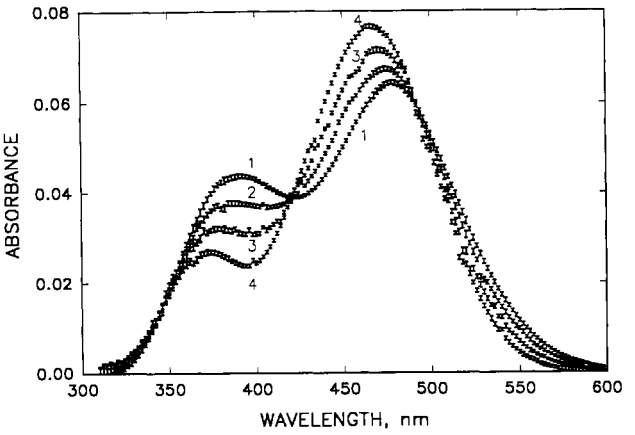

FIGURE 2: Example of 4 spectra selected from a series of 20 corrected postflash difference spectra used for determination of the meta II concentration as a function of time after bleach. Postflash times are (1) 3 s, (2) 3 min, (3) 8.5 min, and (4) 50 min. A well-defined isosbestic point is observed at 422 nm. Error bars are the result of the propagation of the standard deviation of the original data points of the digitized spectra, as determined by the Hewlett-Packard 8452A. Difference spectra were corrected for the absorbance of unbleached rhodopsin as described in *Analysis of Meta II Decay Time* under Materials and Methods.

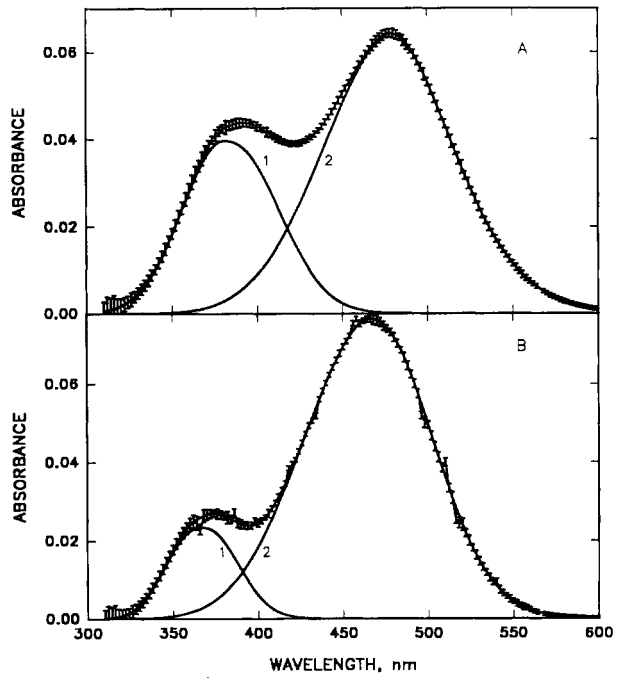

FIGURE 3: (A) Corrected difference spectrum acquired 3-s postflash and fit with a combination of meta I (λ_{max} = 478 nm) and meta II (λ_{max} = 380 nm) bands. The solid curve through the points is the sum of the individual deconvoluted meta II (1) and meta I (2) bands. (B) Corrected difference spectrum acquired 50-min postflash and fit with a combination of meta III (λ_{max} = 465 nm) and NRO_{365} bands. The solid curve through the points is the sum of the individual NRO_{365} (1) and meta III (2) bands.

The criteria for the correctness of fits of photointermediate species to corrected difference spectra were the location of the derived absorption bands and overall mass balance. Mass balance refers to the sum of the concentrations of the derived photointermediates divided by the concentration of bleached rhodopsin. For all fits of photointermediates, the mass balance never varied from 1.0 by more than 5%, and the average mass balance was within 2% of 1.0, as shown in Table I. All fits of the four photointermediate species (meta I, meta II, meta III, and NRO_{365}) to corrected difference spectra resulted in absorbance maxima which were within 2–3 nm of their respective published values, a good level of agreement considering that the original spectra were digitized only every 2 nm. The analytical results were very consistent in terms of the mass balance of photointermediates relative to rhodopsin bleached, the relative amounts of the photointermediates, the location of their absorbance maxima, and the overall quality of the fits of these species to the corrected difference spectra, as illustrated in Figure 3A,B. This consistency clearly demonstrates that the photointermediates present 3-s and 50-min postflash are well characterized as meta I–meta II and meta III–NRO_{365} mixtures, respectively.

Table I: Mass Balance Derived from the Deconvolution of Corrected Difference Spectra into Individual Photointermediate Bands[a]

	meta I + meta II from 3-s scan	meta III + NRO_{365} from last scan	meta I + meta II + meta III + NRO_{365} from scans at intermediate times
average	1.01 ± 0.03	0.98 ± 0.04	1.00 ± 0.04
largest deficit[b]	0.97 ± 0.06	0.96 ± 0.07	0.95 ± 0.07
largest surplus[b]	1.04 ± 0.05	1.03 ± 0.07	1.04 ± 0.08

[a] Concentrations of photointermediates as a fraction of the total rhodopsin bleached. Listed uncertainties correspond to 1 standard deviation. For meta I + meta II and meta III + NRO_{365}, n = 4; for meta I + meta II + meta III + NRO_{365}, n = 72. [b] Largest deficit and largest surplus refer to the individual cases where the sum of the derived photointermediate concentrations yielded the largest under and overestimate, respectively, when compared with the concentration of bleached rhodopsin.

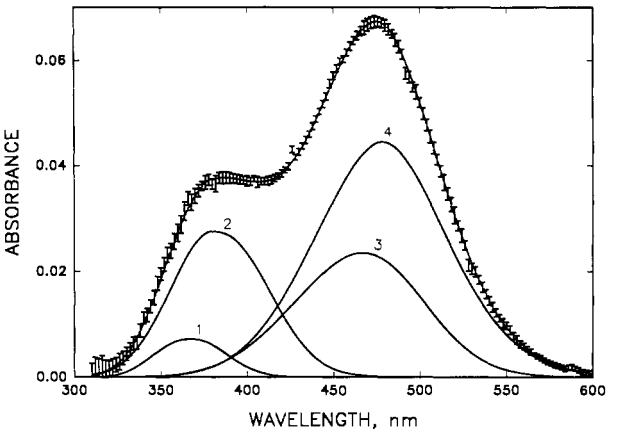

FIGURE 4: Example of the fit of the meta I–meta II and meta III–NRO_{365} absorbance profiles to one of the series of postflash spectra. Points with error bars are the corrected difference spectrum acquired 3-min postflash. The solid curve through the points is the sum of the deconvoluted spectral data resulting from optimizing the contribution due to the meta I–meta II absorbance profile (Figure 3A) and the meta III–NRO_{365} absorbance profile (Figure 3B). Individual bands are NRO_{365} (1), meta II (2), meta III (3), and meta I (4).

In order to accurately assess the decay of meta II, it was necessary to deconvolve the meta II absorption band from each of the approximately 20 postflash corrected difference spectra. This was accomplished by fitting the intermediate spectra with a linear combination of the meta I–meta II and meta III–NRO_{365} absorbance profiles, derived from the 3-s and 50-min spectra, respectively. Plots of the ca. 20 corrected difference spectra for each of 4 independent experiments showed an isosbestic point at 422 nm (see the example in Figure 2). This isosbestic point validates the expectation that the ratios of meta I–meta II and meta III–NRO_{365} remain constant during the observed decay process. A typical example of this type of fit to one of the postflash spectra, along with the resulting deconvolved meta I, meta II, meta III, and NRO_{365} absorption bands, is given in Figure 4. The proper mass balance of photointermediates relative to rhodopsin bleached, which was

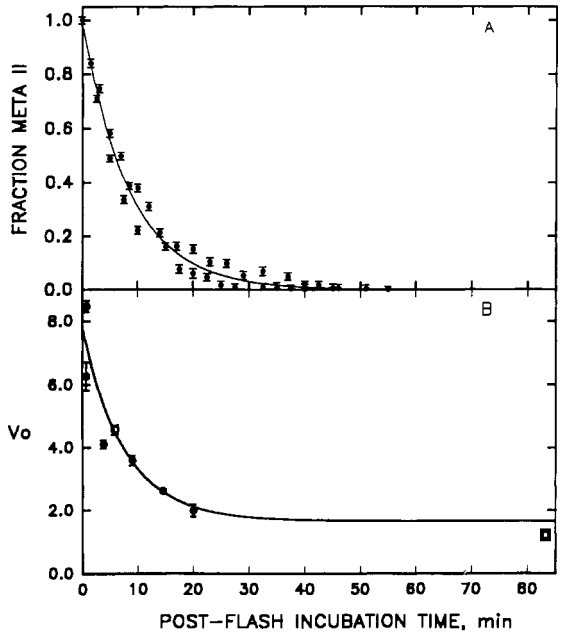

FIGURE 5: Plots of the decay of meta II and rho*. (A) Data points are the absorbance maximum of the deconvoluted meta II spectrum taken at the indicated postflash times. Error bars represent 1 standard deviation and were derived as described in *Analysis of Meta II Decay Time* under Materials and Methods. (B) Decay of rho* as obtained from one of two complete data sets. Error bars represent 1 standard deviation and were derived as described in *Nucleotide Exchange Measurements and Analysis* under Materials and Methods; points without error bars have standard deviations smaller than the symbols. Initial velocities corresponding to points (○) (5.95 min) and (□) (83.23 min) are derived from the nucleotide exchange time courses shown in Figure 6. The curves in (A) and (B) are single-exponential decays fit to the data points by using a nonlinear least-squares procedure.

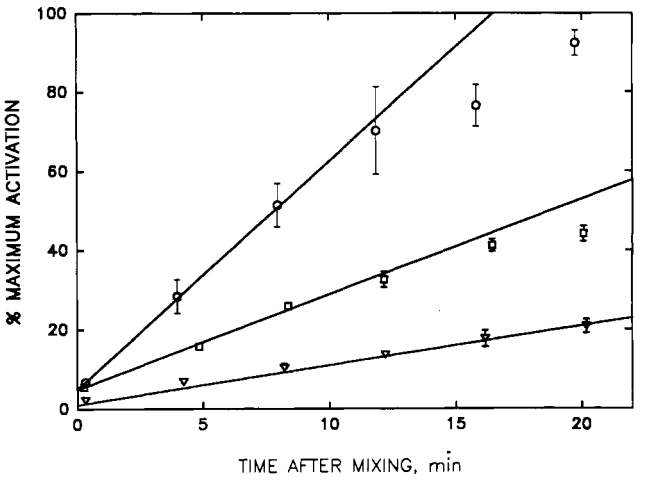

FIGURE 6: Example of nucleotide exchange time courses. Postflash incubation times are as follows: time course 1, (○), 5.95 min (V_0' = 5.77 ± 0.15); time course 2 (□), 83.23 min (V_0' = 2.41 ± 0.13). Time course 3 (▽) represents a dark control (V_d = 0.98 ± 0.05). Units of V_0' and V_d are change in percent maximum exchange per minute. Filter-bound dpm were converted to moles of bound GMPPNP to give a measure of the quantity of G_t activated, assuming one molecule of bound nucleotide per molecule of G_t. V_0 was calculated from V_0' and V_d as described in *Nucleotide Exchange Measurements and Analysis* under Materials and Methods.

observed for the 3-s and 50-min spectra, was maintained in the intermediate spectra, as shown in Table I. For spectral fits of the type shown in Figure 4, the peak positions and band shapes of the individual photointermediates and the ratios of meta I to meta II and meta III to NRO_{365} were held constant. Only the fraction of the derived meta I–meta II spectral profile and the fraction of the derived meta III–NRO_{365} spectral profile were varied to produce the fit to the spectral data shown in Figure 4. All of the intermediate corrected difference spectra were similarly well described by this type of fitting procedure, demonstrating that the mixture of photointermediates in these spectra had been completely characterized. Decay of meta II, as followed by the decrease in its contribution to the total absorbance, is presented in Figure 5A and is determined from the global fit of the meta II spectrum rather than by following the change in absorbance at a single wavelength. Fitting a single-exponential decay to the data using nonlinear least squares gives a decay time of 8.2 min with a standard deviation of 0.5 min (n = 4).

Rho Decay Time.* The decay time of rho* was determined by carrying out nucleotide exchange time courses on aliquots of a disk suspension at various postflash incubation times. Examples of nucleotide exchange time courses from a data set where the bleach level was 0.33%, giving an initial G_t/rho* ratio of 162/1, are shown in Figure 6. At these rho* levels and mixing conditions (no preincubation period with G_t prior to initiation of the nucleotide exchange time courses), the activation profiles of the recombined systems showed subsaturating bleach characteristics, in that rho* was not present in sufficient amounts to give instantaneous, maximal activation as is seen for unattenuated flashes yielding bleaches of ca. 4% (data not shown). As postflash incubation times are increased, the amount of rho* present decreases due to thermal decay. This is illustrated in nucleotide exchange time courses 1 and 2 in Figure 6 [(○) and (□), respectively]. Linear activation behavior persists for a longer period of time in time course 2 (postflash incubation time 83.23 min) than it does in time course 1 (postflash incubation time 5.95 min), since the assay mixture in time course 2 contains less rho*.

The initial velocity of a nucleotide exchange time course was taken to be proportional to the amount of rho* present after that postflash incubation time. V_0' values derived from data of the type shown in Figure 6 were corrected for dark control activity by subtracting V_d. The resulting V_0 values were plotted versus postflash incubation time and fit with a single-exponential decay, as shown in Figure 5B. The decay curve is made up of two components: a dynamic component and a residual component that remains relatively constant after the dynamic process is complete. The decay time for the dynamic component is 7.7 min with a standard deviation of 0.5 min (n = 2), corresponding closely to the decay time determined spectroscopically for meta II.

Meta II ↔ Meta III Reversibility. Failure of the decay curve to return to base line (dark control) levels at times well after the dynamic process is complete suggests either that some residual level of rho* is still present or that some rho* formation can be induced under the assay conditions. We investigated the hypothesis that G_t added at the start of the assay time course bound residual meta II, which was in equilibrium with meta III, thereby perturbing the meta II ↔ meta III equilibrium and increasing the meta II concentration in a manner analogous to the meta II enhancement from meta I. Hypotonic extract, containing no GTP or GTP analogue, was added to samples which had been allowed to decay to meta III over the course of 50 min at 20 °C. Hypotonic extract buffer was added to identical aliquots of meta III containing samples. The addition of G_t at a ratio of 0.8 G_t per bleached rhodopsin induced the formation of meta II, with a corresponding loss of meta III. The control samples, those to which hypotonic extract buffer was added, showed no loss of meta III, remaining basically unchanged for at least 20 min following addition of buffer. A typical example of the spectral

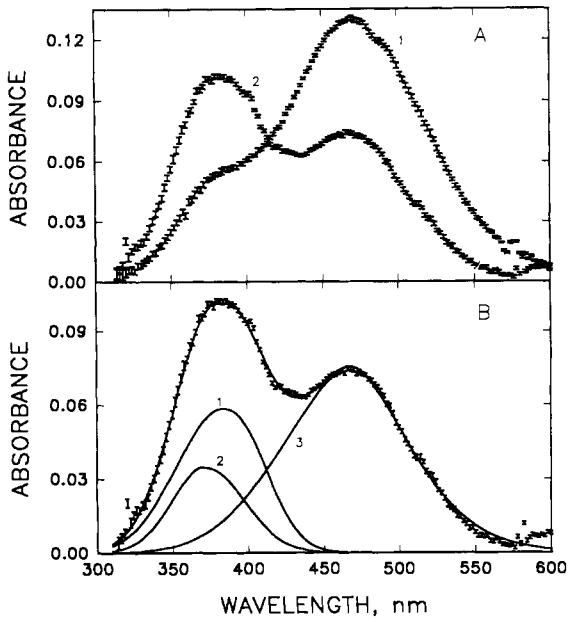

FIGURE 7: Enhanced meta II formation from meta III. (A) Spectra taken 50-min postflash, (1) before and (2) after addition of hypotonic extract containing G_t. (B) Deconvolution of the spectrum resulting from the addition of G_t. The solid curve through the spectral data is the sum of the individual meta II (1), NRO_{365} (2), and meta III (3) bands, derived as described in *Effect of G_t on Meta II–Meta III* under Materials and Methods.

shifts caused by the addition of G_t is shown in Figure 7A, where spectrum 1 is the corrected difference spectrum observed at 50-min postflash and spectrum 2 is the spectrum observed 20 min after the addition of hypotonic extract containing G_t. The spectral shifts induced by added G_t typically stabilized within 10 min, and remained stable for at least 20 min. Under these conditions, no meta I is expected to form, because essentially all meta II is complexed with G_t. In order to deconvolve spectra resulting from the addition of G_t, it was assumed that the addition of G_t lowered the meta III band without changing its shape or location and had no effect on the NRO_{365} band. Thus, this corrected difference spectrum was fit with the exact NRO_{365} band which was deconvolved from the spectrum acquired before addition of G_t, the meta III band which was also determined before addition of G_t, with the height allowed to vary, and an independent asymmetric quasi-Gaussian. The resulting fit to spectrum 2 in Figure 7A is shown in Figure 7B, along with the deconvolved bands for NRO_{365}, meta II, and meta III. For all data sets, the fitting procedure centered the independent quasi-Gaussian at 380 ± 3 nm, with a band shape essentially identical with that previously determined for meta II. Following this deconvolution, published extinction coefficients were used to determine the concentrations of meta II (Applebury, 1984) and meta III (Blazynski & Ostroy, 1984). In all cases, the amount of meta III removed was within 3–4% of the amount of newly formed meta II, indicating that the added G_t, by binding to meta II which was in equilibrium with meta III, induced a shift in the meta II ↔ meta III equilibrium in favor of meta II formation. The amount of meta II formed typically corresponded to ca. half of the added G_t binding meta II to form stable meta II·G_t.

Discussion

The goal of the current studies was to determine if meta II and rho* exist in the same time regime. Direct measurements of the decay times of meta II and of rho* give similar values of 8.2 min (SD = 0.5 min) and 7.7 min (SD = 0.5 min), respectively. This result demonstrates that the meta II absorbance profile serves as an indicator of the persistence of the physiologically active species of photoactivated rhodopsin, rho*, and substantiates conclusions relative to the equivalence of rho* and meta II drawn from less direct findings regarding the correlated formation of meta II and G_t binding capacity. We have previously proposed the existence of two forms of meta II, meta II_{fast} and meta II_{slow}, based on the need for the sum of three exponentials to describe the kinetics of meta II formation (Straume et al., 1990). However, on the time scale of minutes, the decay of meta II is well described by a single exponential, as shown in Figure 5A, and these species appear to be unresolved. The spectrum of meta II reflects the electronic environment of the retinal chromophore in the interior of rhodopsin, while the G_t-activating capacity of rho* reflects the exposure of a G_t binding site at the cytoplasmic surface of rhodopsin. The overall temporal coincidence of meta II and rho* indicates that the conformation of these two regions of the protein—the membrane-buried helices surrounding the chromophore and the cytoplasmic loop regions that interact with G_t—are coupled during both formation and decay of the activating species, in spite of their spatial separation. The slight difference in the observed decay times may reflect the existence of protein conformational substates in the meta II photointermediate, all of which have identical spectra. Rho* may sample a unique or selected group of meta II protein substates, leading to the slight difference in rho* and meta II decay times.

While the meta II decay curve falls essentially to zero, the rho* decay curve reveals a residual level of activity that remains constant after the decay of meta II is complete. This residual activity suggests activation by some photointermediate present after the apparent spectral decay of meta II. In order to clarify the origin of the residual activity, we considered the possibility that the constant residual activity results from the establishment of a reversible meta II ↔ meta III equilibrium. The apparent meta II decay to zero in the spectral measurements shows that this equilibrium must be shifted far toward meta III in the absence of G_t. However, a residual steady-state concentration of meta II at a level of ~5% of the meta III concentration would be unresolved by the spectral analysis employed in these studies. Hence, the addition of G_t at longer postflash incubation times, so as to initiate the activation time courses, could shift a preexisting, reversible meta II ↔ meta III equilibrium toward meta II, just as G_t binding shifts the meta I ↔ meta II equilibrium toward meta II. Approximately equal residual G_t activation was observed in the two rho* decay data sets studied, corresponding to about 23% of initial activation in spite of different G_t/rho* ratios of 162/1 and 387/1, suggesting that all the recoverable meta II had already been converted at the lower G_t concentration. The observed increase in meta II absorbance coupled with the loss in meta III absorbance in the presence of added G_t can only be explained by stabilization by G_t of meta II formed from the meta III pool. This result provides the first direct evidence for a dynamic meta II ↔ meta III equilibrium, first suggested by Chabre and Breton (1981). It is difficult to quantitatively compare the estimated rho* concentration that would generate an exchange velocity equal to 23% of the initial postflash exchange velocity, and the concentration of meta II produced via G_t enhancement because of the following differences in conditions between the two measurements. The exchange and enhancement studies were carried out at different G_t/bleached rhodopsin ratios (>160/1 and 0.8/1, respectively). The exchange time courses measured activation of G_t in the presence of a nonhydrolyzable GTP analogue, and the uptake of the

analogue by G_t removes available G_t from the substrate pool. The enhancement experiments measured binding of G_t in the absence of a GTP analogue, and were thus done under constant G_t concentrations and stable binding conditions. In spite of these experimental differences, the results confirm in a qualitative sense that the residual rho* activity seen in the exchange measurements stems from G_t-driven rho* formation.

The residual activity and meta II enhancement from meta III observed in the experiments might have some bearing on the results reported by Okada et al. The presence of low levels of meta III in their samples may account for the apparent G_t activation by photointermediates other than meta II. However, the GTPase activity observed after the addition of hydroxylamine, which ought to have converted meta III to retinal oxime plus opsin, is not explained by our results.

It is well established that binding of G_t to meta II induces a near-complete shift in the meta I $\leftrightarrow$ meta II equilibrium in favor of meta II (Emeis & Hofmann, 1981; Emeis et al., 1982; Kibelbek et al., 1991). However, the addition of G_t shifts the meta II $\leftrightarrow$ meta III equilibrium to only about equal concentrations of meta II and meta III. This striking difference in G_t enhancement of meta II may be understood in terms of the relative free energies of the species meta I, meta II, meta III, and G_t·meta II. The change in free energy is calculated from the equilibrium constant according to $\Delta G^\circ = -RT \ln K_{eq}$. The results of the present work show that meta II is 0.2 kcal/mol higher in free energy than meta I and meta III is 0.2 kcal/mol lower in free energy than the G_t·meta II complex. The results of a recent set of experiments with rhodopsin in POPC vesicles at 20 °C, pH 8.0, indicate that the G_t·meta II complex is $\sim$2 kcal/mol lower in free energy than meta II (Kibelbek et al., 1991). This $\sim$2 kcal/mol represents the binding energy of G_t to meta II. G_t binds to the exposed cytoplasmic surface of rhodopsin; therefore, it is reasonable to assume that the binding energy is not strongly influenced by the composition of the surrounding bilayer. Given this assumption, it is possible to combine the G_t binding energy determined in POPC vesicles with the change in free energy for G_t·meta II $\rightarrow$ meta III determined in ROS disk membranes to obtain an estimate of the change in free energy for meta II $\rightarrow$ meta III. The result of this calculation is that meta III is about 2.2 kcal/mol lower in free energy than meta II. This corresponds to a meta II $\leftrightarrow$ meta III K_{eq} of 44 and accounts for the fact that no meta II is observed in the meta III sample prior to addition of G_t. The detection limit of the experiment is such that meta II could be resolved when the meta II $\leftrightarrow$ meta III equilibrium has a K_{eq} of 19, and meta III is 1.8 kcal/mol lower in free energy than meta II. These thermodynamic considerations show that the differences in the degree of enhancement of meta II are due to the fact that meta I is $\sim$2.0 kcal/mol higher in free energy than meta III. The difference in free energy between meta I and G_t·meta II is -1.8 kcal/mol, while between meta III and G_t·meta II it is $+0.2$ kcal/mol. Thus, it is not surprising that G_t induces a relatively modest shift from meta III to G_t·meta II but induces a nearly complete shift from meta I to G_t·meta II.

The similarity of decay times demonstrates the functional equivalence of meta II and rho*, since no other photointermediates exists in the time domain defined by the decay time of rho*. Therefore, the presence of meta II serves as an indicator of the G_t-activating conformation of photoactivated rhodopsin. The relatively slow time scale for the thermal decay of the activating conformation and the ability to form meta II from meta III in the presence of G_t suggest that shut-off mechanisms other than thermal decay must be operative to inactivate meta II, the equivalent of an agonist-bound receptor in this system. Thus, under physiological conditions, the regulatory mechanism of phosphorylation coupled with 48K protein would be required for sensitive yet transient signaling in visual transduction (Miller et al., 1986; Wilden et al., 1986).

ACKNOWLEDGMENTS

We thank Dr. James L. Miller for helpful discussions concerning sample preparations and the nucleotide exchange assay and Deborah L. Stokes for excellent technical assistance.

REFERENCES

Applebury, M. L. (1984) *Vision Res. 24*, 1445–1454.
Bennett, N., Michel-Villaz, M., & Kuhn, H. (1982) *Eur. J. Biochem. 127*, 97–103.
Blazynski, C., & Ostroy, S. E. (1981) *Vision Res. 21*, 833–841.
Blazynski, C., & Ostroy, S. E. (1984) *Vision Res. 24*, 459–470.
Chabre, M., & Breton, J. (1979) *Vision Res. 19*, 1005–1018.
Deterre, P., Bigay, J., Forquet, F., Robert, M., & Chabre, M. (1988) *Proc. Natl. Acad. Sci. U.S.A. 85*, 2424–2428.
Emeis, D., & Hofmann, K. P. (1981) *FEBS Lett. 136*, 201–207.
Emeis, D., Kuhn, H., Reichert, J., & Hofmann, K. P. (1982) *FEBS Lett. 143*, 29–34.
Fung, B. K.-K. (1985) in *Molecular Mechanisms in Transmembrane Signalling* (Cohen & Houslay, Eds.) pp 183–214, Elsevier Science Publishers B. V., Amsterdam, The Netherlands.
Fung, B. K.-K., & Stryer, L. (1980) *Proc. Natl. Acad. Sci. U.S.A. 77*, 2500–2504.
Hofmann, K. P. (1985) *Biochim. Biophys. Acta 810*, 278–281.
Hofmann, K. P. (1986) *Photochem. Photobiol. 13*, 309–327.
Johnson, M. L. (1983) *Biophys. J. 44*, 101–106.
Johnson, M. L., & Frasier, S. G. (1985) *Methods Enzymol. 117*, 301–342.
Kibelbek, J., Beach, J. M., & Litman, B. J. (1990a) *Biophys. J. 57*, 367a.
Kibelbek, J., Beach, J. M., & Litman, B. J. (1990b) *10th International Biophysics Congress Abstracts*, p 481, National Research Council of Canada, Ottawa, Canada.
Kibelbek, J., Mitchell, D. C., & Litman, B. J. (1991) *Biophys. J. 59*, 533a.
Kuhn, H., Bennett, N., Michel-Villaz, M., & Chabre, M. (1981) *Proc. Natl. Acad. Sci. U.S.A. 78*, 6873–6877.
Longstaff, C., Calhoon, R. D., & Rando, R. R. (1986) *Proc. Natl. Acad. Sci. U.S.A. 83*, 4209–4213.
Mathews, R. G., Hubbard, P. K., & Wald, G. (1963) *J. Gen. Physiol. 47*, 215–240.
McDowell, J. H., & Kuhn, H. (1977) *Biochemistry 16*, 4054–4060.
Miller, J. L., Fox, D. A., & Litman, B. J. (1986) *Biochemistry 25*, 4983–4988.
Miller, J. L., Litman, B. J., & Dratz, E. A. (1987) *Biochim. Biophys. Acta 898*, 81–89.
Miller, J. L., Hubbard, C. M., Litman, B. J., & Macdonald, T. L. (1989) *J. Biol. Chem. 264*, 243–250.
Okada, D., Nakai, T., & Ikai, A. (1989) *Photochem. Photobiol. 49*, 197–203.
Parkes, J. H., & Liebman, P. A. (1984) *Biochemistry 23*, 5054–5061.
Straume, M., Mitchell, D. C., Miller, J. L., & Litman, B. J. (1990) *Biochemistry 29*, 9135–9142.
Stryer, L. (1986) *Annu. Rev. Neurosci. 9*, 87–119.
Wilden, U., Hall, S. W., & Kuhn, H. (1986) *Proc. Natl. Acad. Sci. U.S.A. 83*, 1174–1178.